Water Research 224 (2022) 119053

Contents lists available at ScienceDirect

Water Research

journal homepage: www.elsevier.com/locate/watres

# In flux: Annual transport and deposition of suspended heavy metals and trace elements in the urbanised, tropical Red River Delta, Vietnam

Lucy R. Roberts [a,b,*], Nga T. Do [c,d], Virginia N. Panizzo [a], Sarah Taylor [a], Michael Watts [e], Elliot Hamilton [e], Suzanne McGowan [a,f], Duc A. Trinh [c], Melanie J. Leng [g,h], Jorge Salgado [a]

[a] Centre for Environmental Geochemistry, School of Geography, University of Nottingham, Nottingham, NG7 2RD, UK
[b] Department of Ecoscience, Aarhus University, C. F. Møllers Allé 4-6, 8000 Aarhus, Denmark
[c] Nuclear Training Center, Vietnam Atomic Energy Institute, 140 Nguyen Tuan, Thanh Xuan, Hanoi, Vietnam
[d] Electric Power University, 235 Hoang Quoc Viet, Cau Giay, Hanoi, Vietnam
[e] British Geological Survey, Keyworth, Nottingham, NG12 5GG, UK
[f] Department of Aquatic Ecology, Netherlands Institute of Ecology, Droevendaalsesteeg 10, 6708 PB Wageningen, The Netherlands
[g] National Environmental Isotope Facility, British Geological Survey, Keyworth, Nottingham, NG12 5GG, UK
[h] Centre for Environmental Geochemistry, School of Biosciences, University of Nottingham, Sutton Bonington Campus, Loughborough LE12 5RD, UK

ARTICLE INFO

*Keywords:*
Elemental flux
Suspended particulate matter
Anthropogenic pollution
Sediment transport
Tropical deltas

ABSTRACT

Due to the depositional environment, river deltas are said to act as filters and sinks for pollutants. However, many deltas are also densely populated and rapidly urbanizing, creating new and increased sources of pollutants. These sources pose the risk of tipping these environments from pollution sinks to sources, to the world's oceans. We provide detailed seasonal and annual assessments of metal contaminants in riverine suspended particulate matter (SPM) across the densely populated Red River Delta (RRD), Vietnam. The global contributions of elements from the RRD are all <0.2% with many elemental fluxes <0.01%, suggesting the RRD is not a major source of elemental pollution to the ocean. However, 'hotspots' of metal pollution due to human activity and the impacts of tropical storm Son Tinh (July 2018) exceed both national level regulations and international measures of toxicity (e.g. enrichment factors). There is widespread 'extreme pollution' of Cd (enrichment factor >40) and concentrations of As higher than national regulation limits (>17 mg/Kg) at all sites other than one upstream, agricultural-dominated tributary in the dry season. These 'hotspots' are characterised by high inputs of organic matter (e.g. manure fertiliser and urban wastewater), which influences elemental mobility in the particulate and dissolved phases, and are potentially significant sources of pollution downstream. In addition, in the marine and fresh water mixing zone, salinity effects metal complexation with organic matter increasing metals in the particulate phase. Our calculations indicate that the delta is currently acting as a pollutant sink (as determined by high levels of pollutant deposition ~50%). However, increased in-washing of pollutants and future projected increases in monsoon intensity, saline intrusion, and human activity could shift the delta to become a source of toxic metals. We show the importance of monitoring environmental parameters (primarily dissolved organic matter and salinity) in the RRD to assess the risk of transport and accumulation of toxic metals in the delta sediments, which can lead to net-increases in anthropogenic pollution in the coastal zone and the incorporation of toxic elements in the food chain.

## 1. Introduction

Large rivers are the main source of eroded material into the world's oceans, with 70% of global suspended particulate matter (SPM) derived from rivers in southern Asia, the large Pacific and the Indian Ocean Islands (Viers et al., 2009). Riverine SPM comprises inorganic (e.g. clay-minerals and iron-manganese [Fe-Mn] oxyhydroxides) and organic (detritic or living) matter and is the primary carrier of heavy metals in fluvial systems. Large Asian rivers are therefore important in global biogeochemical cycles and the transport of pollutants through watersheds. On average, >90% of riverine SPM is deposited in estuaries and deltas (Martin and Whitfield, 1983), making south and southeast Asian

* Corresponding author.
*E-mail address:* l.roberts@ecos.au.dk (L.R. Roberts).

https://doi.org/10.1016/j.watres.2022.119053
Received 15 March 2022; Received in revised form 1 September 2022; Accepted 2 September 2022
Available online 3 September 2022

mega-deltas a potentially significant sink of pollutants.

The primary sources of metals in riverine SPM are from atmospheric deposition, weathering of catchment materials, and anthropogenic inputs (e.g. agricultural runoff). The textural composition and organic matter of sediments is critical in determining the sorption and complexation of transition metals (Jenne 1968; Warren and Zimmerman 1994), with the mineralogy and grain size of silts and clays predominantly carrying metal contamination from upstream (e.g. Roy et al., 2018). The amount of SPM delivered by rivers therefore depends on: 1) natural catchment controls including relief, surface-area, geology, vegetation type and cover, and climate (temperature, precipitation, runoff, intensity and number of flood events); and 2) anthropogenic activities and catchment modifications including industry, agriculture, land cover, and the diversion of flow. Furthermore, sediments are transported downstream or deposited as bottom sediments, but natural (e.g. flooding) and anthropogenic (e.g. dredging) activities can lead to

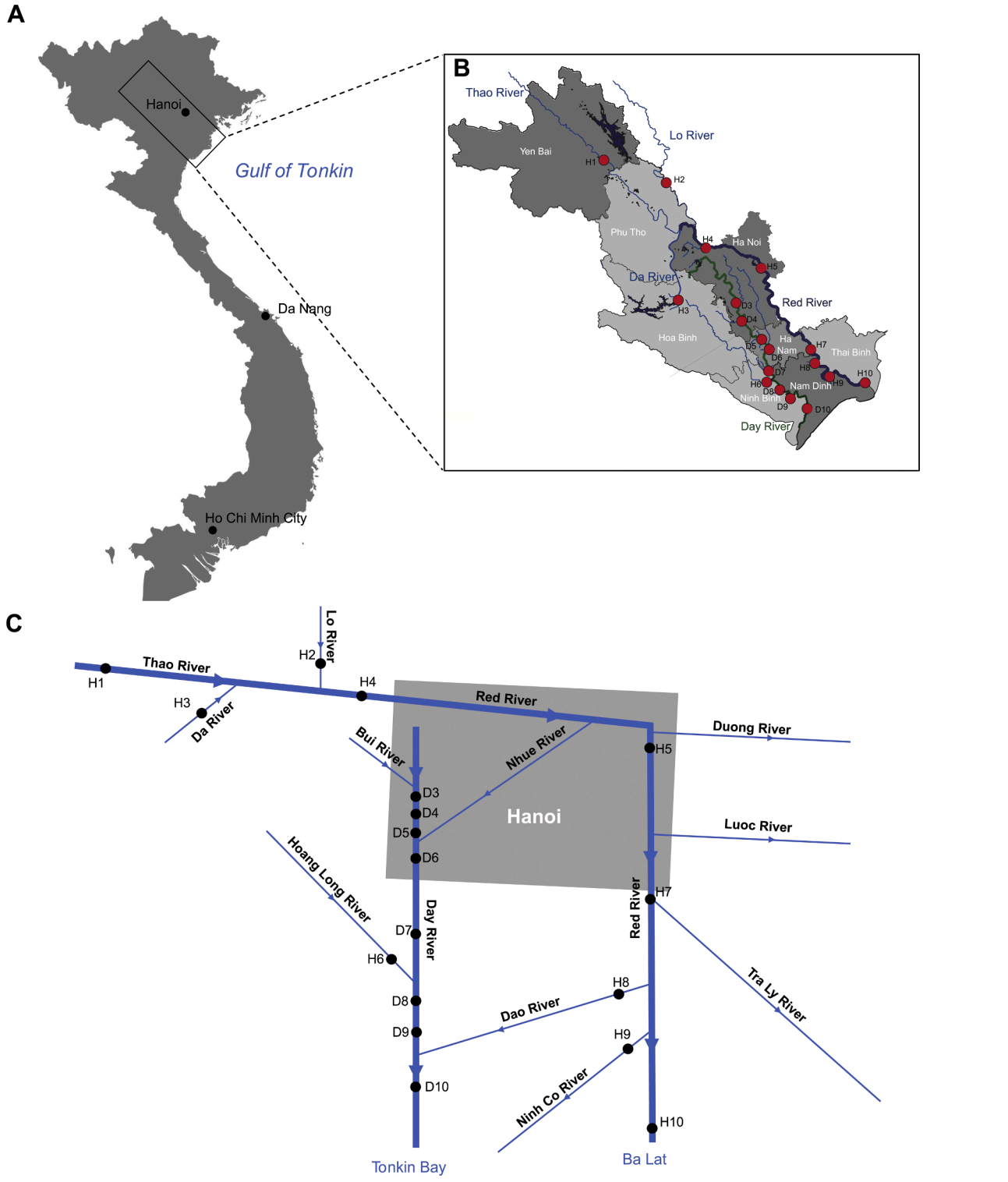


**Fig. 1.** Location of the Red River Delta in Northern Vietnam (a) and the sampling locations within the Red River Delta (b). A schematic of the Red River Delta (c) allows the hydrological network to be seen more clearly.

their resuspension.

Asian mega-deltas, such as the Red River Delta (RRD) in Vietnam, deliver 30% of global suspended sediment to the oceans (Samanta and Dalai, 2018). Excess sediment in coastal environments can lead to increased turbidity with negative impacts on endangered benthic marine organisms, such as coral reefs, and increases in the net contribution of anthropogenic pollutants to the coastal zone. Asian mega-deltas are some of the most densely populated and urbanizing environments in the world (Ericson et al., 2006; Woodroffe et al., 2006), increasing the input of suspended matter and pollutants to the coast. However, estimates of annual fluxes of pollutants through such deltas are still limited. Here we provide the first detailed, multi-seasonal assessment of river SPM elemental composition and contamination for the RRD, Vietnam.

### 1.1. The red river delta

The RRD, northern Vietnam, is the fourth largest delta in Southeast Asia spanning 14,300 $km^2$ (Fig 1). The monsoonal climate (annual rainfall 700–4800 mm $yr^{-1}$) has a rainy season from May to October (up to 80% of rainfall) and a dry season from November to April. SPM is therefore highly seasonal (Le et al., 2020). The delta is situated < 3 m above sea level and throughout the Quaternary, eustatic sea-level changes have shifted the boundary between fluvial- and marine- dominated environments. Today, tidal effects can be seen in river levels at Phu Ly (located close to D6; Fig 1c) and during the dry season, they can extend up to Hanoi (H5; Fig 1c; Minh et al., 2014). The fluvial network of the delta is dense (2–4 km/$km^2$) extending 1126 km from the source in China to the mouth at Ba Lat estuary (Tran, 2007). On entry to Vietnam, the river known as the Thao River, receives water from the Da River and the Lo River. It enters the deltaic area as the Red (Hong) River at Son Tay (H4; Fig. 1), where it then divides to the Day River and Duong River. The Duong River flows eastwards and drains out of the delta area (Fig. 1c). The main channel continues to flow through Hanoi to Ba Lat (Fig. 1). The Day River to the right of the main channel has a length of 240 km and a watershed area of ~8500 $km^2$. Of river discharge, 21% is derived from the upper Red River in China, with 54% and 25% derived from the Da and Lo Rivers respectively. However, an estimated 78% of SPM is eroded from upstream in China (Ha and Coynel, 2016).

The dense river network with easy access to water has encouraged settlement, with a population of >21 million, growing annually by 1.14% (General Statistic Office 2018, 2020), and a rapid increase of industry and agriculture. In 2017, 37% of land was used for agriculture (General Statistic Office, 2017) and there were 731 traditional so-called "craft villages" specialising in a variety of industries, including textiles, food processing, ceramic works, and recycling plants (Mahanty et al., 2012). Waste products from domestic activities, agriculture, and industry (including nutrients and heavy metal pollution) enter the river network unregulated and untreated (Quynh et al., 2005; Luu et al., 2012; Mahanty et al., 2012). Consequently, air and water pollution in 90% of craft villages throughout Vietnam exceed the limits required under the law on Environmental Protection (MONRE, 2008; The World Bank, 2008; EPA, 2009).

With a monitoring record covering 21 years, since 2000 (Trinh et al., 2009), the RRD is one of the best studied tropical river systems. Whilst industrial and agricultural pollution of the RRD are well studied and often quantified (e.g. Luu et al., 2012; Mahanty et al., 2012; Ha and Coynel, 2016), there is minimal information on seasonal and annual fluxes of suspended elements through the catchment. Elements in the dissolved phase (e.g. Cr) from mining and craft villages have been documented (Mahanty et al., 2012) around Hanoi and the bioaccumulation of metals (Zn, Cu and Cd) has been quantified for the Nhue-Day River basin (Ngo et al., 2021). However, potential widespread pollution due to the transport, resuspension, and deposition of SPM across the delta remains largely unknown. Previous work has focused on either the Red (e.g. Le et al., 2018) or Day-Nhue catchments (e.g. Do and Nishida, 2014; Do et al., 2019; Luu et al., 2020; Ngo et al., 2021). High suspended sediment fluxes in the Red River in combination with numerous pollution sources lead to a high proportion of trace metals in the particulate phase (Trinh et al., 2013). Therefore, we aimed to provide a more complete overview of sediment and pollutant flux from 18 locations across the RRD over a 18-month period (from February 2018 to July 2019), quantifying the annual fluxes of pollutants in the RRD and its contribution to global biogeochemical cycles for the first time.

## 2. Methods

### 2.1. Field collections

Eighteen sampling points were located at key parts of the Red (10 stations) and Day-Nhue rivers (8 stations), covering a range of land uses (Table 1) to characterise spatial and temporal trends in sediment delivery and metal contamination across the RRD; sites are labelled as H and D respectively. Upstream site H1 is located at the Thao River after the river enters Vietnam from China. The delta starts at Son Tay (H4) and the river flows through the east side of Hanoi City at H5 (Fig. 1). The upstream catchment (H1-H4) has a low population density (< 100 inhabitant $km^2$) and high forest cover (Le et al., 2020). The remaining portion of the catchment has a very high population density (>1000 inhabitant $km^2$), intensive agriculture, and urban pollution (Le et al., 2020). The Nhue River receives wastewater from Hanoi City (H5) and enters the Day River upstream of D6 (Fig. 1), introducing further potential contaminants into the Day River. In addition, the expansion of hydropower and associated impoundments in the catchment has reduced sediment delivery (Le et al., 2020) and introduced the potential for downstream storage of contaminants from urban and agricultural wastewater.

The 18 locations were sampled monthly between February 2018 and July 2019 (Fig. 1) across a range of land uses (Table 1). At each location water was sampled at 50 cm depth and filtered using GF/F (0.7 μm) filter papers. Between 300–1000 ml of water was filtered until adequate suspended sediment was retained on the filter paper (Table S1). Filter papers were pre-weighed and ashed at 550 °C prior to collection. Two filter papers were retained for the calculation of total suspended solids (TSS) and heavy/ trace metal concentration. For analysis of major ions to characterise waters of marine composition, a 30 ml aliquot of filtered water was retained and stored at <10 °C. To permit a comparison of upstream contaminant storage in the RRD catchment and examine the effects of impoundment on the transport of elements, core-top sediments (0–1 cm) from a 61 cm sediment core collected from Hoa Binh reservoir in 2017 were retained for ICP-MS analysis.

**Table 1**
Summary of land use for each sampling location.

| Site | River | Land Use | Hydro-Meteorology station |
|---|---|---|---|
| D3 | Day | Urban + Agriculture | Ba Tha |
| D4 | Day | Agriculture | Ba Tha |
| D5 | Day | Agriculture | Ba Tha |
| D6 | Day | Urban + Agriculture | Phu Ly |
| D7 | Day | Agriculture | Phu Ly |
| D8 | Day | Agriculture | Gian Khau + Phu Ly |
| D9 | Day | Urban + Agriculture | Gian Khau + Phu Ly |
| D10 | Day | Agriculture | Gian Khau + Phu Ly + Nam Dinh |
| H1 | Hong | Urban | Yen Bai |
| H2 | Lo | Mining | Vu Quang |
| H3 | Da | Mining | Hoa Binh |
| H4 | Hong | Agriculture | Son Tay |
| H5 | Hong | Urban | Hanoi |
| H6 | Hoang Long | Urban | Gian Khau |
| H7 | Tra Ly | Agriculture | Quyet Chien |
| H8 | Dao | Agriculture | Nam Dinh |
| H9 | Ninh Co | Agriculture | Truc Phuong |
| H10 | Hong | Agriculture | Ba Lat |

### 2.2. Hydrological data

To calculate the element fluxes of particulate matter in the RRD, daily river discharge ($m^3/s$) was obtained from nine hydrological stations in the upstream (sites H1-H3) and downstream (sites H4, H5, H7, H8, H9, H10) reaches of the Red River. There are no hydrological stations recording river discharge in the right branch of the Red River, or the Day-Nhue River Basin (D sites). Instead, four stations record daily water level (cm): Ba Tha (D3), Phu Ly (D6), Gian Khau (H6) and Nhu Tan (D10). Water level data were provided by the centre of Hydro-Meteorology (HMD, Vietnam centre for Hydro-Meteorological Data; http://cmh.com.vn/en/). To derive discharge for 2018–2019, the water level-discharge relationships in Luu et al. (2010) were used. To investigate the seasonal patterns in discharge across the delta, z-scores were calculated to compare amongst sites. A z-score calculates the standard deviation relative to the mean, to standardize the data and allow seasonal patterns to be highlighted. A monthly z-score was calculated for each hydrological station, and subsequently used to generate a mean z-score for the RRD as a whole, using the following equation:

$$Z = \frac{x - \mu}{\sigma} \quad (1)$$

Where $x$ is the hydro-meteorology station monthly mean discharge, $\mu$ is the RRD mean annual discharge, and $\sigma$ is the standard deviation of RRD annual discharge.

### 2.3. Water ionic composition

To delineate the marine influence, and therefore the effects of salinity on element partitioning, dissolved major ions ($Na^+$, $Mg^+$, $K^+$, $Ca^+$, $Cl^-$ and $SO_4^{2-}$) were analysed. Filtered waters were analysed by ion chromatography according to the methods described in APHA (2017) and corrected for cyclic salts. Total alkalinity was determined by the single-point titration method using methyl orange as a colouring indicator according to methods described in Clesceri et al. (1999).

### 2.4. Total suspended sediment (TSS)

Filter papers were dried at 105 °C for 24 hrs and weighed after cooling in a desiccator. TSS values, including organic matter, were then calculated as follows:

$$\mathrm{TSS}\ \left(\mathrm{mg\ L^{-1}}\right) = \frac{(\mathrm{Weight_1\ (mg)} - \mathrm{Weight_2\ (mg)})\ \mathrm{x}\ 10^3}{\mathrm{Volume\ (ml)}} \quad (2)$$

Where $Weight_1$ is the final weight of the filters, and $Weight_2$ is the initial dry weight of the filter.

TSS is monitored daily at the national hydro-meteorology stations (Yen Bai, Hoa Binh, Vu Quang, Hanoi and Ba Lat; Table 1) using the same filtration method and 1 L of water. Monthly averages and one standard deviation of TSS were calculated from these daily measurements and compared with our one-off monthly value. In most cases, our value falls within one standard deviation of their mean monthly TSS value, suggesting our data are representative of monthly TSS. Since the values are representative, the hydro-meteorology station TSS is not available at all sites, and the method is most comparable to the collection of SPM for elemental analysis, our monthly measurements of TSS were used for the calculation of elemental fluxes.

Daily SPM elemental fluxes were calculated using daily hydro-meteorology station TSS data at the appropriate stations to provide an idea of the variability in flux calculations (Text S1). TSS fluxes were not calculated based on our TSS data because the 2019 sampling period only covered half of the year (until July 2019) and modelling the data for the remainder of the year would introduce uncertainty into the calculation, whereas the hydro-meteorology station TSS provides daily data for the full 12 months, providing a more accurate calculation of flux. Furthermore, the use of the hydro-meteorology station data allowed comparison with historical trends.

### 2.5. Suspended particulate matter (SPM) geochemistry

#### 2.5.1. Heavy and trace metal concentrations

Filter papers were freeze-dried and weighed directly into microwave vessels, to which 5 ml of concentrated $HNO_3$ and 0.1 ml HF was added. Vessels were left to settle for 30 min before sealing. The vessels were heated via a ramping programme to 200 °C using a CEM Mars microwave system, cooled before venting (to prevent the release of volatiles e.g. Si) and 0.5 ml of $H_2O_2$ added. Heating, cooling, and venting was repeated for a second cycle before solutions were transferred to Savellex containers and dried gently at <90 °C overnight on a hotplate. The residue was reconstituted with 1 ml concentrated $HNO_3$, heated for 30 min at 30 °C and made up to a total volume of 10 ml with deionised water. Blank filters were analysed with each microwave batch for subsequent blank correction after analysis. Two additional blank filters were 'spiked' with a certified reference material NIST 2584 within each microwave batch as a measure of reproducibility and accuracy for the dissolution stage. Analysis of sample solutions was undertaken using an Agilent 8900 series ICP-QQQ-MS. To overcome polyatomic interferences, the ICP-MS collision cell was operated in He mode at a flow rate of 5.5 ml $min^{-1}$ for all elements except P and As; for these elements, $O_2$ was introduced into the cell at a flow rate of 30%, in conjunction with MS/MS determination, to measure the oxide product ion (e.g. $^{75}As^{16}O^+$). Quality control (QC) standards were analysed at the start and end of each run and after no more than every 20 samples.

#### 2.5.2. Annual flux estimation

January to December is defined here as the annual cycle to allow comparison with previous work in the RRD (e.g. Luu et al., 2010; Le et al., 2020) and to give equal weighting to wet and dry seasons of 6 months each. Annual fluxes of TSS were calculated using the daily hydro-meteorology station data and the calculation used in Le et al. (2020):

$$\mathrm{Flux}\ \left(10^6 \mathrm{tyr^{-1}}\right) = \frac{\sum C_i Q_i \left(24\ \times\ 60\ \times\ 60\ \times\ 10^{-6}\right)}{10,000,00} \quad (3)$$

Where i is the day of year, $C_i$ is the discrete instantaneous concentration ($mg\ L^{-1}$) on a given day, $Q_i$ is the corresponding daily discharge ($m^3/s$).

To establish the degree of anthropogenic influence or geogenic origin of heavy and trace elements, enrichment factors (EF) were calculated for each element:

$$\mathrm{EF\ (X)} = \frac{\mathrm{X/Al_{sample}}}{\mathrm{X/Al_{UCC}}} \quad (4)$$

Where EF (X) is the enrichment factor of the given element (X), and X/Al is the concentration of the selected element normalised to the concentration of Al in the sample. Upper Continental Crust (UCC) values were taken from Taylor and McLennan (1985), McLennan (2001), Rudnick and Gao (2003), and Hu and Gao (2008). To determine the degree of anthropogenic enrichment, the contamination categories of Sutherland (2000) were used (Text S2). EF values were also calculated for the global average SPM and a range of Asian rivers (Text S1).

Where the average SPM EF value across the catchment for the sampling period was below 2, suggesting geogenic origin, the element is excluded from further discussion, but is presented alongside other flux calculations. Annual SPM metal fluxes were calculated for each sampling location using:

$$\mathrm{Flux}\left(10^3 \mathrm{tyr^{-1}}\right) = \left(\left(\mathrm{C_d\ x\ TSS_d}\right)\ \mathrm{x}\ Q_d\right)\ \mathrm{x}\ 0.0846 \quad (5)$$

Where $C_d$ is the concentration (mg/Kg) of a given element on the sampling day, $TSS_d$ is the total suspended sediment on the given sampling

day (mg $L^{-1}$), $Q_d$ is the daily discharge ($m^3/s$) and 0.0846 is the conversion factor to tonnes. The measured TSS from the field collected filter paper was used in this equation to best reflect the SPM concentration collected at the same time. This was calculated for each sampling day and regression curves using a power function $Flux = aQ^b$ (Table S3) were developed to estimate fluxes for the remaining days. The annual flux was the sum of daily fluxes, which could then be compared to other tropical rivers and used to calculate inflow and outflow (Text S2).

## 3. Results

### 3.1. Hydro-meteorology station discharge

Mean monthly RRD discharge varies seasonally with peak discharge during the wet season (May to October; Fig. 2a). Discharge between 2018 and 2019 was highly variable across the catchment (Fig. 2b), which is reflected in the high standard deviations in monthly RRD z-score discharge (Fig. 2a). Over the sampling period, the highest and most variable discharges were recorded at Son Tay (Fig. 2b). Variability in discharge was lowest at Ba Tha, Gian Khau and Phy Ly located on the Day River (D sites; Fig 2b). Discharge was lower in 2019 than 2018 at all hydro-meteorology stations other than Ba Lat, located at the mouth of the Hong River. The seasonality in mean RRD discharge is also displayed in the mean monthly discharge at each hydro-meteorology station (Fig. S2, Text S3)

### 3.2. Marine versus freshwater influence

Dissolved ionic composition of waters from H10 (Hong River), in the lower part of the delta, sit in the hydrochemical space of $Na^+$-$K^+$-$Cl^-$

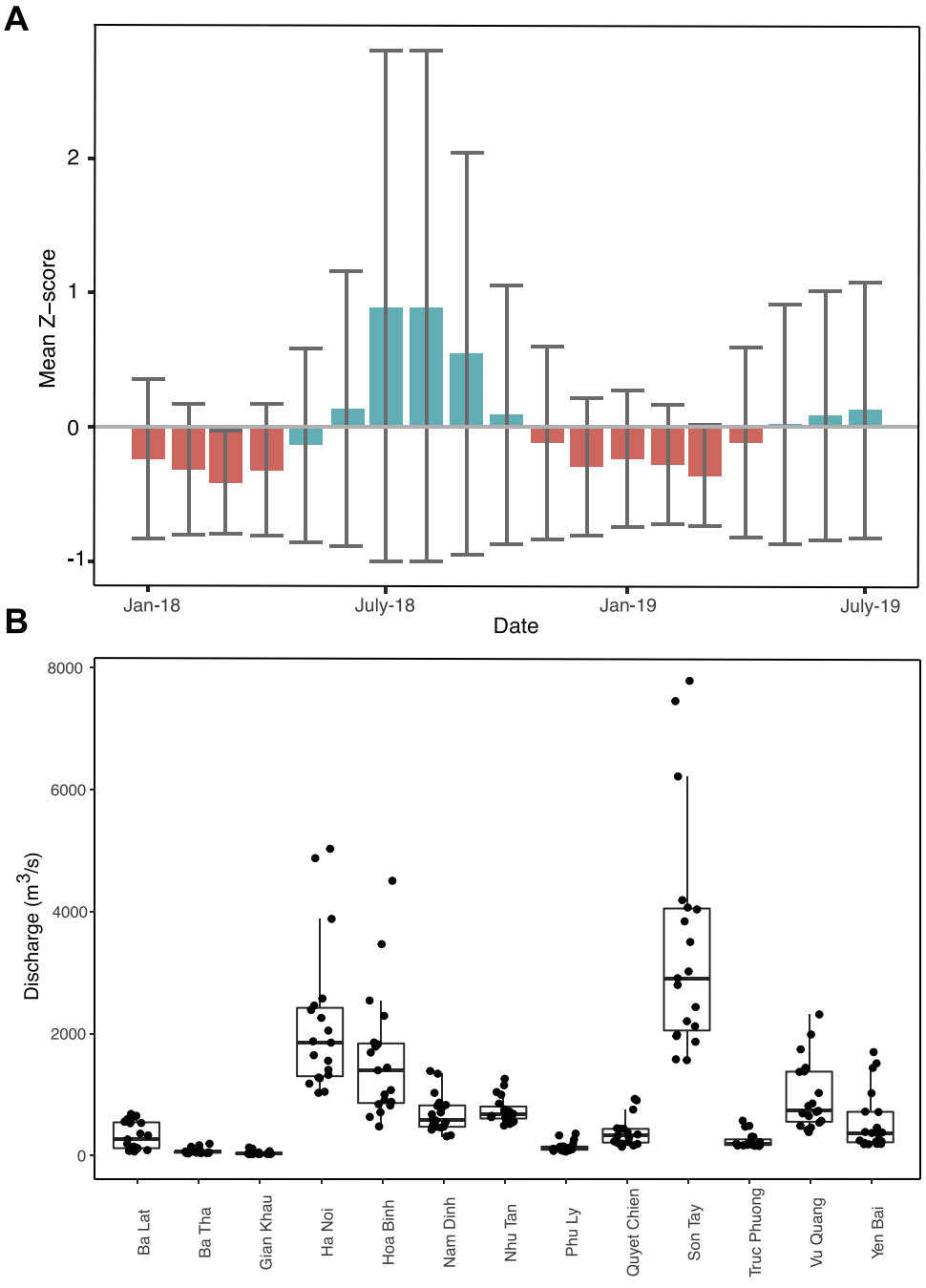


**Fig. 2.** Variability in discharge for the hydro-meteorology stations across the RRD with a) z-scores used to standardize the discharge amongst stations to investigate the seasonal patterns and b) boxplots of monthly variation between sites; the black dots represent monthly mean values per site and are jittered across the x-axis to prevent overlap. The mid-line represents the median, the lower and upper hinges correspond to the 25th and 75th percentiles and the upper/lower whisker extends to the largest/smallest value no further than 1.5* the inter-quartile range.

dominance, typical of marine waters (Fig. 3). In contrast, the remaining sites were $Ca^{2+}$ dominated and are typical of freshwaters. Marine or freshwater ionic composition was unaltered during the wet and dry seasons, other than in January 2019 (dry season) at D10, at the mouth of the Day River, when waters were of marine composition, suggesting some saline intrusion with reduced freshwater inflow (Fig. 3).

### 3.3. TSS concentrations

From our sampling, average TSS concentrations were highest at the most upstream site, H1 (an annual average of 152.59 ± 114.81(1σ) mg $L^{-1}$ in 2018 and 114.37 ± 124.87 mg $L^{-1}$ in 2019), and lowest at H3 (annual averages of 9.10 ± 9.20 mg $L^{-1}$ and 4.81 ± 6.39 mg $L^{-1}$), located on the Da River tributary (Table 2). TSS concentrations were often highest in the wet season (Table 2) except for in a few sites in the mid-delta (D7, D8 in 2019, D10 in 2019, and H6 in 2018). It is important to note that our sampling for 2019 only covers January to July and therefore the values are not directly comparable to 2018, which covers February to December (for monthly concentrations, consult Table S4). Daily TSS concentrations at hydro-meteorology stations are not used in the calculation of elemental fluxes but concentrations were compared to see if one-off monthly sampling precisely reflected monthly TSS. In most cases, our value falls within one standard deviation of their mean monthly TSS value. For detailed comparison see Text S4.

### 3.4. Metal concentration of SPM

Seasonal trends in suspended metal concentrations were spatially variable across the RRD catchment (Fig. S3, Text S5). For metal concentrations in riverine sediments, the Vietnamese National Technical Regulation on Sediment Quality sets limits for Cr, Cu, As, Cd, and Pb (Table S7; QCVN 43:2017/BTNMT). Concentrations of As were high at all sites across the RRD, exceeding the QCVN limits for at least two months of the year in both the wet and dry seasons (Fig. 4). In general, concentrations were lowest in H3 (the Da River flowing from Hoa Binh reservoir) whereas concentrations exceeded limits for sediments in both fresh and brackish waters at numerous sites in the Day River (D sites). For Cr, Cu, Cd, and Pb, concentrations at most sites were below the limits set by QCVN (Fig. 4) with the exception of the upstream site of H1 during the dry season (March and April) in 2018. In March 2019, concentrations of Cu were close (within 10 mg/Kg) to the limit. Particulate concentrations of Cr were more distinctively seasonal, with concentrations above QCVN limits in the wet season (June to October) at all sites other than H1 (furthest upstream) and H10 (at the mouth of the river).

Strong significant positive correlations ($p$ <0.001) were observed in both the wet and dry seasons between Fe and Ti ($r$ = 0.933 and 0.910), in the wet season between P and Mn ($r$ = 0.943) and Cr and Cd ($r$ = 0.939), and in the dry season between Cr and Cu ($r$ = 0.998) and Cd and Pb ($r$ = 0.961). Significant ($p$ <0.005), but weak, negative correlations ($r$ = < –0.4) were observed between: P and Ti; P and Fe; Ti and Cr; Ti and Mn; Ti and Cd; Cr and Fe; Mn and Fe; Mn and Ba; Fe and Cd; and Cd and Ba. These negative correlations were observed in wet and dry seasons.

#### 3.4.1. Enrichment factors

Average RRD EF values for Mg, K, Ca, and Ti were below 2, suggesting geogenic origin. However, values for some locations suggest moderate (Mg, K, Ca, Ti) localised pollution, primarily around sites D5 to D7 (located around Hanoi; Fig. 5). Enrichment factors for four elements (Mn, As, Cd, Ba) were >40 at one location, suggesting extreme pollution. Average RRD EF values were >40 (extreme pollution), and above the global average value, for Cd and Ba. Cd values were >40 at all sites in the RRD and were above the global average at H1, H5, H8 and D5; the highest average EF of 933 at D5 (Hanoi) suggests high localised pollution. For Ba, values for all sites in the RRD were higher than the average global and Asian values. An EF value of 137 for Ba at H3 (located on the tributary flowing from Hoa Binh reservoir) suggests a pollution hotspot. There are several elements where EF values indicate moderate pollution but were lower than the average values for Asian rivers, including Ni (average RRD EF of 4) and Pb (average RRD EF of 7). For all elements, the EF values for core-top sediments in Hoa Binh were lower than the average value for the RRD, suggesting significant anthropogenic pollution downstream. However, EF values highlight moderate pollution of Cr, Mn, Ni, and Cu, significant pollution of As, and extreme pollution of Cd.

### 3.5. Annual fluxes of TSS and elements

Annual fluxes of TSS estimated from the hydro-meteorological station data for Yen Bai (H1), Vu Quang (H2), Hoa Binh (H3), Hanoi (H5), and Ba Lat (H10) are presented in Table 3. Unlike our sampling data, the TSS data from the hydro-meteorology station is available for all months of 2018 and 2019. The highest annual flux was estimated for H1 furthest upstream with 23.5 × $10^6$ tonnes $yr^{-1}$ in 2018 and the lowest at Hoa Binh of 0.3 × $10^6$ tonnes $yr^{-1}$ in 2019. The annual TSS flux in 2019 was lower at all hydro-meteorology stations. When compared with previous data from Le et al. (2020), the TSS flux for Yen Bai in 2018 is

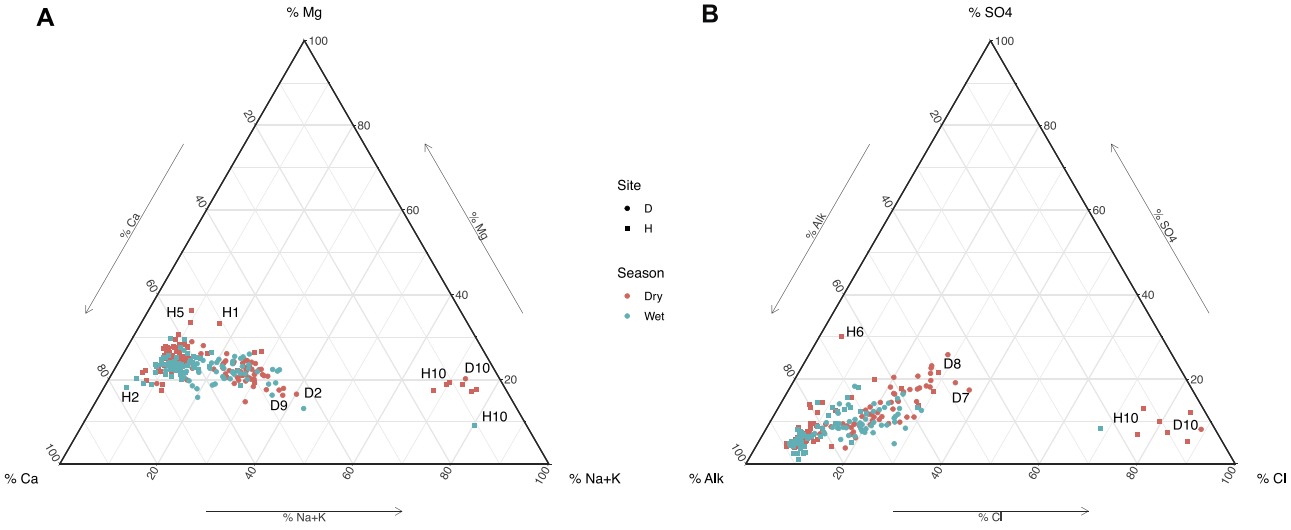


**Fig. 3.** Ternary plots of major cation (a) and anion (b) composition of waters. Waters of marine composition are situated in the lower right hydrochemical space of Na-K-Cl dominance.

**Table 2**
Annual and seasonal total suspended solid concentrations for each sampling site. Note that our sampling for 2019 does not cover a full year and therefore the values are not directly comparable to 2018 (i.e. for 2019, the wet season does not include August, September and October and the dry season does not include November and December). Comparisons for months where data are available for 2018 and 2019 are presented in Table S4.

| | Concentration mg $L^{-1}$ | | | | | | | | | | | |
|---|---|---|---|---|---|---|---|---|---|---|---|---|
| | 2018 | | | | | | 2019 | | | | | |
| | Annual | ± 1σ | Wet | ± 1σ | Dry | ± 1σ | Annual | ± 1σ | Wet | ± 1σ | Dry | ± 1σ |
| D3 | 32.53 | 18.84 | 35.13 | 25.83 | 29.42 | 5.59 | 26.14 | 6.44 | 27.17 | 6.63 | 25.37 | 7.19 |
| D4 | 23.40 | 16.65 | 31.98 | 18.14 | 13.11 | 6.26 | 13.57 | 3.25 | 15.50 | 3.54 | 12.12 | 2.49 |
| D5 | 22.96 | 11.21 | 22.27 | 2.31 | 23.79 | 17.48 | 15.01 | 10.56 | 22.18 | 12.62 | 9.64 | 5.18 |
| D6 | 22.52 | 16.41 | 26.27 | 18.71 | 18.02 | 13.75 | 10.30 | 7.07 | 14.36 | 8.39 | 7.25 | 4.92 |
| D7 | 31.32 | 20.87 | 26.88 | 18.98 | 36.64 | 23.95 | 23.96 | 6.17 | 22.52 | 6.90 | 25.04 | 6.39 |
| D8 | 39.66 | 34.64 | 31.87 | 27.07 | 49.02 | 43.40 | 38.03 | 13.57 | 33.81 | 14.36 | 41.19 | 14.13 |
| D9 | 28.48 | 13.05 | 30.08 | 16.87 | 26.56 | 7.86 | 20.82 | 8.06 | 21.88 | 1.58 | 20.03 | 11.24 |
| D10 | 80.82 | 133.34 | 122.57 | 175.63 | 30.72 | 11.79 | 21.91 | 13.59 | 21.93 | 4.97 | 21.90 | 18.79 |
| H1 | 152.59 | 114.81 | 207.60 | 107.24 | 60.47 | 66.34 | 114.37 | 124.87 | 189.00 | 159.35 | 58.40 | 67.14 |
| H2 | 17.30 | 11.82 | 21.37 | 12.88 | 13.59 | 8.59 | 17.22 | 13.33 | 27.08 | 16.32 | 9.83 | 2.75 |
| H3 | 9.10 | 9.20 | 12.88 | 10.30 | 7.21 | 8.71 | 4.81 | 6.39 | 9.13 | 8.51 | 1.57 | 0.84 |
| H4 | 26.94 | 11.84 | 31.11 | 10.18 | 18.02 | 12.51 | 45.57 | 45.80 | 49.38 | 50.62 | 42.71 | 49.61 |
| H5 | 74.11 | 68.68 | 107.20 | 71.78 | 40.94 | 37.69 | 103.52 | 139.53 | 81.67 | 46.53 | 119.91 | 191.47 |
| H6 | 35.19 | 27.52 | 24.73 | 9.75 | 46.82 | 35.46 | 28.90 | 11.38 | 37.98 | 12.03 | 22.08 | 4.24 |
| H7 | 39.11 | 34.09 | 49.28 | 40.39 | 28.84 | 17.68 | 19.07 | 6.46 | 19.11 | 8.49 | 19.03 | 5.95 |
| H8 | 33.01 | 25.98 | 45.52 | 26.31 | 16.32 | 9.41 | 15.00 | 10.23 | 22.56 | 7.32 | 9.33 | 8.58 |
| H9 | 30.68 | 22.63 | 42.90 | 21.72 | 16.07 | 8.46 | 17.39 | 5.70 | 17.78 | 4.33 | 17.10 | 7.23 |
| H10 | 40.75 | 23.99 | 45.28 | 22.55 | 101.76 | 153.53 | 25.42 | 6.40 | 27.47 | 3.78 | 23.89 | 8.06 |

anomalously high compared with the 2010–2019 period, but 2019 is more similar to fluxes between 2010 and 2015 at $9.2 \times 10^6$ tonnes $yr^{-1}$ (Table 3). For Vu Quang and Hoa Binh, the 2018 and 2019 flux shows a steady decline since 2010–2015, in agreement with previous trends.

Higher fluxes of all elements in particulate form were exported from the Hong River than the Day River and fluxes were substantially higher in 2018 (Table 4). Higher fluxes of Li, Mg, K, Ca, Cu, and As were associated with the upper delta, whereas fluxes of Al, P, Ti, Cr, Mn, Fe, Ni, Cd, Pb were higher in the middle delta. Annual fluxes of Cu, Ba, C and N were highest in the lower section of the delta. Fluxes of Li, Mg, P, Ti, Cr, Mn, Fe, Ni, Cu, As, Cd, Ba, and Pb decreased between the upstream and middle section of the delta before increasing at D10 and H10 where the delta is influenced by marine waters (Fig. 6). Fluxes of all elements were highest in the upstream section of the delta (H1-H5) with fluxes at H4 and H5 (around Hanoi) being substantially higher for most elements (Fig. 6). The elemental flux entering the delta (at D6, H6, and H4) was lower than that exported (from D10, H9, H10, H7 and Thuong Cat), by an average of 48.08% in 2018 and 50.46% in 2019. The greatest increases were exhibited by Mg (87.27% in 2018 and 86.85% in 2019) and least by Cr (29.48%) and Ca (20.26%) in 2018 and 2019 respectively (Table 5).

When comparing the monthly mean fluxes calculated using the daily TSS versus those calculated using our monthly field data, flux data sometimes potentially over- or underestimates monthly elemental flux by not accounting for variability in TSS (Fig. S4). Primarily these occasions are associated with anomalous events that are not possible to model. For example, we underestimated metal flux in July 2018 when very high daily flux values were associated with the in-wash of materials from storm Son Tinh. Most of the Son Tinh rainfall across the RRD was recorded during the 18th and 19th of July. Our elemental data (based on the daily TSS) is highest on July 20th and 21st. Our monthly sampling took place before the storm (15th July) and therefore does not capture the elevated TSS from this event. In addition, we overestimated monthly flux at H10 during June and July 2019. This is related to the increase in discharge at Ba Lat in 2019, compared with 2018 (Fig. S2).

## 4. Discussion

### 4.1. Changes in sediment flux since 2000

Since SPM in rivers is a primary carrier of metal contaminants (which can be toxic), the amount of TSS is an important measure for understanding elemental fluxes through catchments. For the RRD, the TSS data from 2018 to 2019 measured at the hydro-meteorology stations confirms the previously identified continuing decline (Le et al., 2020) in sediment delivery to the delta since the last century (Table 3). The increased construction of dams in both Vietnam and China between 2000 and 2015 has significantly reduced sediment delivery (Ha and Vu, 2012; Le et al., 2020). The data presented here updates estimates of sediment delivery (based on Le et al., 2020) through the delta to include the major city of Hanoi (H5) and Ba Lat (H10) at the mouth of the delta. TSS fluxes around Hanoi in the mid-delta (at H5) are higher than upstream (H3), corroborated by higher organic fluxes into the river around the city of Hanoi (Trinh et al., 2009). However, a decline in sediment flux in the lower part of the delta (H10, Ba Lat), implies subsequent deposition and retention in the delta further downstream. As observed between 1990 and 2015 (Le et al., 2020), TSS fluxes were lowest in the Da River (H3), which flows from Hoa Binh reservoir (Fig. 1; Table 3), confirming the impacts of the dam construction on sediment retention along the river (Hoa Binh was constructed in 1989). The upstream dam and reservoir, Hoa Binh, is therefore likely to be acting as a barrier limiting sediment delivery, and potential upstream sources of pollution, downstream.

Compared with 2010–2015, TSS fluxes were higher at all sites in 2018. This TSS increase is likely due to increased precipitation in 2018 (~20% higher than in 2019; Nguyen et al., 2021) which was due to the July 2018 tropical storm Son Tinh. This storm resulted in large scale flash flooding and mudslides around Yen Bai (H1), Hoa Binh (H3), Hanoi (H5) and Nam Dinh (H8) (Davies, 2018; Wright, 2018). Increased TSS fluxes are therefore likely related to the in-wash of eroded material from the delta, rather than an increase in sediment delivery from upstream. Higher concentrations of elements such as Li and Ti, which are associated with weathering and terrestrial soils, in July to August at D3, D6-D10, H3, H5-H8 support this interpretation (Fig. S3).

### 4.2. Spatial trends in element concentrations

Whilst the dam at Hoa Binh reservoir is impacting sediment delivery, the low EF values of core-top sediment impounded in the reservoir (Fig. 5) suggest that pollution is occurring downstream of the dam and that the storage of sediment in Hoa Binh is currently of low environmental health risk. Models for anthropogenically-derived pollution downstream of dams conclude that nutrient (total nitrogen and total phosphorus) fluxes increase overall in the coastal zone even when

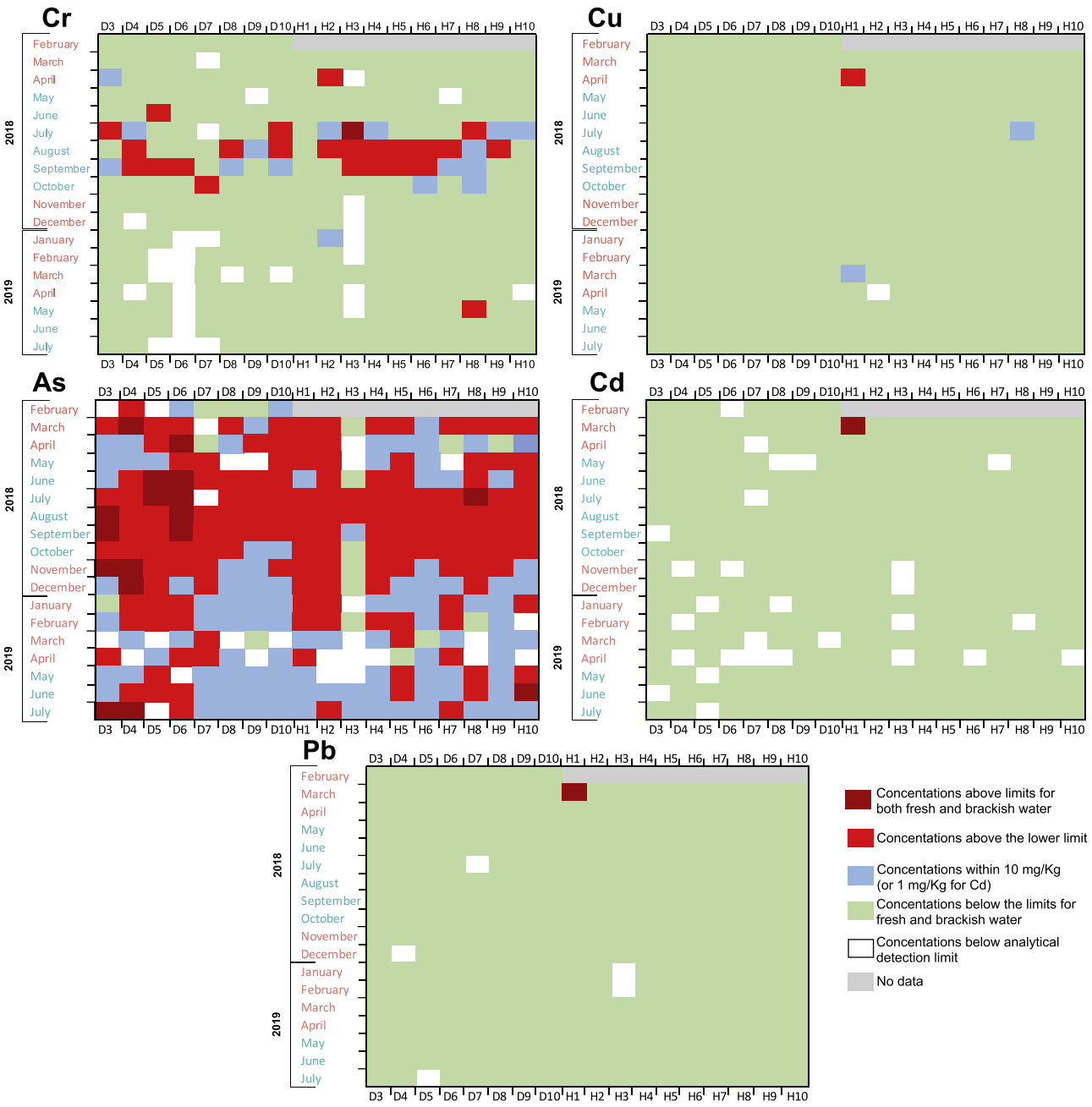


**Fig. 4.** Heatmap for exceedance of Vietnamese National Technical Regulation on Sediment Quality limits for Cr, Cu, As, Cd, and Pb throughout the sampling period. Months of the wet season are highlighted in blue with months of the dry season in red.

concentrations in reservoirs remain low (see Maavara et al., 2020 for an overview).

Several pollution 'hotspots' that exceeded national level regulations and global measures of toxicity were identified downstream in the RRD (Fig. 4 and 5). Unlike other large rivers (e.g. Dupré et al., 1996), elemental composition of SPM in the RRD varies distinctively amongst different locations. Tropical storm Son Tinh in July 2018 exacerbated local pollution due to increased TSS and in-washing, but across both years this spatial structure in SPM suggests localised lithological and chemical influence across the RRD drainage basin and/or the influence of anthropogenic land use modifications. Understanding the source of SPM and heavy metal pollutants in the RRD is therefore an important step in implementing effective riverine ecosystem water quality policy in the catchment.

Correlation analysis can provide insights into the source and/or biogeochemical properties of elements (e.g. Zhang et al., 2018). Here, several significant relationships were observed between small groups of elements, suggesting numerous different sources of pollution. For example, P and Mn are correlated, as are Fe and Ti, which suggests that the sources of P/Mn differ from Fe/Ti. The correlations between these elements could be indications of the Fe phases controlling transportation (e.g. Fe hydroxide nanoparticles or ferrihydrite), which is not captured by our monitoring study. However, despite this limitation, using the approach of Zhang et al. (2018) and the enrichment trends depicted in Fig. S1, high concentrations of these elements at locations with differing land use can assist in identifying major sources of pollution in the RRD. Highest concentrations of P were observed at D6 (downstream Hanoi) during the wet season while highest concentrations of Fe were observed at H8 (in the lower delta) during the wet season. Agriculture is a dominant land use in both locations, but D6 also receives a large amount

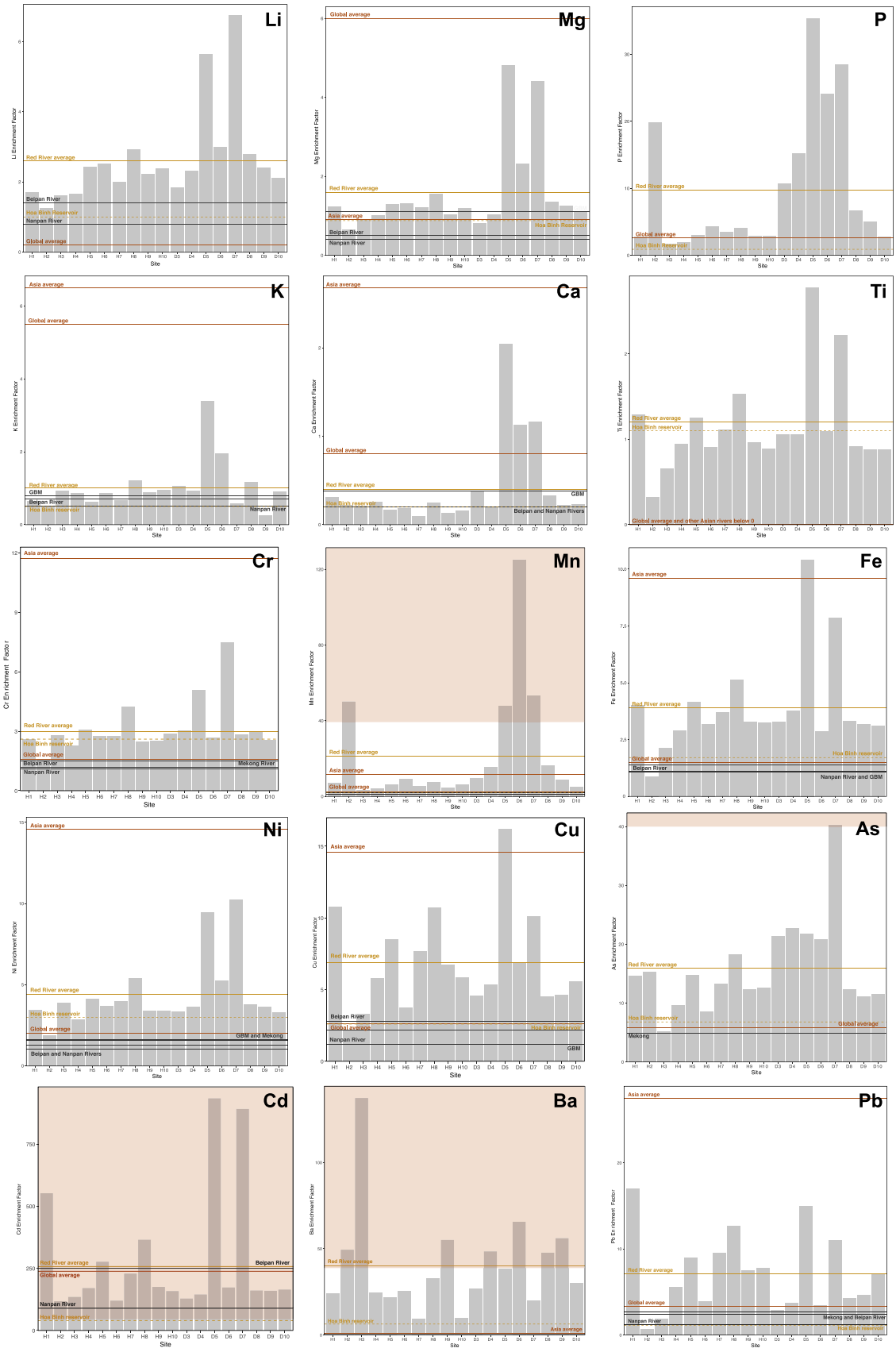


**Fig. 5.** Average enrichment factor (EF) values for each element at the sampling sites. The horizonal lines denote EF values for the Red River average (yellow), background concentrations in Hoa Binh Reservoir (yellow), the global average (orange), Asian river average (orange), Ganges-Brahmaputra-Meghna Delta (black), Mekong Delta (black), Nanpan and Beipan Rivers (black). Red shading indicates an EF above 40 (extreme pollution). Note the different y-axis scales.

**Table 3**
The annual flux of total suspended solids from points along the Red River from this study (2018 and 2019), in comparison to the previous study of Le et al. (2020). The flux of TSS from this study is calculated using data downloaded for the hydro-meteorology stations for January to December for 2018 and 2019 respectively.

| Total Suspended Solid ($10^6$ t $yr^{-1}$) | | | | | | | | | |
|---|---|---|---|---|---|---|---|---|---|
| | Annual mean ± 1σ from Le et al., 2020 | | | | | | | This study | |
| Hydro-meteorology station | Sampling site | 1960–1969 | 1970–1979 | 1980–1989 | 1990–1999 | 2000–2009 | 2010–2015 | 2018 | 2019 |
| Yen Bai | H1 | 34 ± 18 | 38 ± 12 | 36 ± 25 | 59 ± 23 | 41 ± 21 | 7 ± 1 | 23.5 | 9.2 |
| Vu Quang | H2 | 8 ± 3 | 10 ± 4 | 9 ± 4 | 12 ± 3 | 8 ± 5 | 2 ± 1 | 2.7 | 1.7 |
| Hoa Binh | H3 | 57 ± 24 | 53 ± 16 | 32 ± 19 | 7 ± 2 | 5 ± 3 | 1 ± 0 | 0.7 | 0.3 |
| Hanoi | H5 | | | | | | | 13.8 | 6.3 |
| Ba Lat | H10 | | | | | | | 1.8 | 0.7 |

of untreated wastewater from Hanoi via the Nhue River and is located close to the industrial 'craft villages', suggesting wastewater is an important source of P to the catchment (Luu et al., 2012, 2020). Luu et al. (2020) have provenanced the major source of dissolved organic matter (DOC) to be wastewater during the non-fertilisation period (April and October). High levels of DOC increase the complexation between metals and SPM (Shafer et al., 1997). Our findings suggest concentrations of Cd and Cu were also observed at H1 (furthest upstream) during the dry season, where the main land uses are agricultural and urban. During low flows, there is limited dilution of wastewater from urban areas, and therefore the complexation of Cd and Cu with DOC (Zhang et al., 2018) may exacerbate peak concentrations associated with wastewater in the dry season. PCA biplots further suggest the correlation of the enrichment of Cd and Cu, and Mn and P.

During the wet season (July), Luu et al. (2020) found that agricultural sources linked to manure fertilisation in the Day River are the predominant source of organic matter. During this period, they observed high [DOC] at D8, D9, and D10 (but did not include the area covering our 'H' sites). We found high concentrations of Cr at D10 in July to September (during the wet season; Fig. S3), where agriculture is the primary land use. Cr could be supplied by in-wash of agricultural and aquaculture fertilisers, pesticides, and algaecides as documented in the Indian Ganges-Brahmaputra-Meghna Delta (Mitra and Ghosh, 2014). The influence of organic matter from wastewater and manure fertilisation on the complexation of Cd, Cu, and Cr in the RRD should therefore be of concern to the region.

Studies examining the relationships between DOC, SPM, and elemental partitioning ($K_D[Cu]$, $K_D[Cd]$, and $K_D[Pb]$) suggest that Cd has affinities for both DOC and silt/clay-dominated SPM while Cu displays relatively low partitioning in high-clay environments, which could account for the widespread high EF values of Cd compared to the low Cu values. The effects of domestic and industrial inputs along the Nhue River, increases in dissolved organic matter, and the consequent eutrophication (Luu et al., 2020) and increase in Cr, Cd, and Pb (Trinh et al., 2013) are well documented in the Day River. However, our results suggest that the large input of organic matter is also important for the mobilisation of toxic metals at a catchment-wide scale. In addition, concentrations of As are higher than QCVN limits (>17 mg/Kg) at all sites other than H3 in the dry season. Arsenic-rich groundwater is well documented in the RRD (e.g. Agusa et al., 2005), but riverine transport of As is not often considered. The presence of DOC and Fe-oxides, which is the primary component of suspended sediment in the RRD (Trinh et al., 2013), can lead to higher dissolved As (Redman et al., 2002). Enrichment trend analysis (Fig. S1) suggests enrichment of As and P to align, corroborating that wastewater could be a significant contributor of this enrichment. A reduction in inputs of DOC from wastewater could, therefore, significantly improve dissolved and particulate pollution.

Trinh et al. (2013) suggested that the treatment of wastewater to remove organic matter from Hanoi would result in the sorption of heavy metals to suspended sediment rather than organic material, resulting in the deposition and storage of metals in the delta. An estimated 75% of suspended sediment is retained in the delta (Luu et al., 2012) with most deposition occurring in the upper delta (before H4) between Phu Tho and Son Tay (Ha and Coynel, 2016). Most deposition therefore theoretically occurs before the locations that have been identified here as major pollution hotspots (D5, D6, and D7). Due to a lack of hydro-meteorology station TSS data for the Day River, there is still limited understanding of sediment transport. However, our concentration data suggest that the Day River also acts as a source with concentrations remaining high throughout, unlike the Hong River where high/low hydro-meteorological station fluxes are also evident in our concentration data (Table 2). Furthermore, a systematic reduction in sediment delivery to the delta each year (Table 3) will limit transportation and deposition of SPM-bound metals, potentially increasing dissolved concentrations. In addition, the partition coefficient of Cd ($K_D[Cd]$) gradually decreases above 5 PSU (Turner, 1996), suggesting the solubility of SPM-bound Cd in higher salinity areas of the delta might cause further pollution downstream. The removal of organic matter from wastewater will therefore not be the only requirement to limit the transportation of heavy metals from pollution hotspots.

### 4.3. Comparison with global and Asian elemental fluxes

There are limited annual flux estimations from other tropical river systems for comparison, but values for the RRD, even considering uncertainty in variability, are similar to the Paraíba do Sul River system in Brazil (Table 4). The average annual discharge of the RRD across the sampling period accounts for 0.07% of average global river discharge (Dai and Trenberth, 2002). The global contributions of elements from the RRD are all <0.2% with fluxes of Ba contributing most. Most elemental fluxes are all <0.01%, suggesting the RRD is not a major source of elemental pollution to the ocean. The contribution of Ba may appear high in relation to the discharge. Due to the limited comparative data for tropical rivers, we cannot say with a degree of certainty whether this flux is higher than would be expected. However, Ba and Ca correlate on PCA biplots (Fig. S1b,c) suggesting a co-variance potentially associated with the weathering of limestone. For comparison, using the discharge estimates given in Ovalle et al. (2013), the annual average discharge of the Paraíba do Sul are similar, accounting for 0.05% of global river discharge, but elemental fluxes are proportionately higher than the RRD. The difference may be accounted for by the deposition of material in the much larger and older deltaic environment of the RRD compared with the Paraíba do Sul delta, where a larger area of the delta is prograding (Murillo et al., 2009). Progradation results in lower sediment accumulation than where a large delta plain has formed and could account for more export to the oceans (Hori, 2021). This suggests that the RRD deltaic fan is effectively filtering and retaining sediments.

Despite clear evidence of sediment deposition in the RRD, the flux of elements suggests higher concentrations being exported from the delta than entering. Around 78% of SPM derives from upstream in China (Ha and Coynel, 2016) and a high level of sediment retention occurs in the mid- and lower-delta between H5 and H10 (Luu et al., 2010). However, high fluxes in the lower delta suggest that most pollution is occurring in the delta itself. In some instances, there is a low percentage increase between the input and output despite areas of significant pollution (EF above 5) occurring downstream at D5 and D6. For example, the lowest percentage increase in 2018 is in the flux of Cr, suggesting deposition has taken place further downstream in the Day River. In general, fluxes

**Table 4**

Annual fluxes of elements in the Red River Delta in comparison with other tropical river systems (the Ganges-Brahmaputra and Paraíba do Sul; Subramanian et al., 1987; Carvalho et al., 2002) and global fluxes (Viers et al., 2009). annual fluxes were calculated for the Red River (H sites, except H6), Day River (D sites and H6), the upper delta (H1, H2, H3), the mid-delta (H4, H5, H7, D3, D4, D5, D6) lower delta (H8, H9, H10, D7, H6, D8, D9, D10), and the RRD as a whole (sum of all the locations). The Red River Delta contribution to global cycles is estimated using the global flux.

| Elemental Flux(Tonnes $10^3$ $yr^{-1}$) | | | | | | | | | | | | | | | | | | |
|---|---|---|---|---|---|---|---|---|---|---|---|---|---|---|---|---|---|---|
| Red River Delta | | | | | | | | | | | River system | | | | | Global contribution of RRD | | |
| | Red | | Day | | Upper | | Middle | | Lower | | Whole | | Ganges-Brahmaputra | Paraíba do Sul | Global flux | % | | |
| | 2018 | 2019 | 2018 | 2019 | 2018 | 2019 | 2018 | 2019 | 2018 | 2019 | 2018 | 2019 | | | | 2018 | 2019 | |
| Li | 0.06 | 0.02 | 0.00 | 0.00 | 0.03 | 0.01 | 0.02 | 0.01 | 0.01 | 0.01 | 0.06 | 0.02 | | | 128 | 0.049 | 0.019 | |
| Mg | 6.64 | 2.69 | 1.24 | 1.01 | 4.02 | 1.19 | 1.41 | 0.98 | 2.45 | 1.54 | 7.88 | 3.71 | | | 189,000 | 0.004 | 0.002 | |
| Al | 54.66 | 25.43 | 4.83 | 3.24 | 20.34 | 6.85 | 24.55 | 11.86 | 14.67 | 10.05 | 59.50 | 28.71 | | | 1,308,000 | 0.005 | 0.002 | |
| P | 0.89 | 0.47 | 0.16 | 0.11 | 0.25 | 0.10 | 0.41 | 0.23 | 0.38 | 0.25 | 1.05 | 0.58 | | | 30,158 | 0.003 | 0.002 | |
| K | 36.33 | 10.09 | 2.15 | 1.40 | 20.52 | 4.81 | 11.87 | 3.47 | 6.11 | 3.25 | 38.48 | 11.51 | | | 253,500 | 0.015 | 0.005 | |
| Ca | 21.61 | 5.34 | 0.70 | 0.36 | 17.73 | 3.52 | 2.78 | 1.26 | 1.80 | 0.92 | 22.31 | 5.70 | | | 388,500 | 0.006 | 0.001 | |
| Ti | 2.18 | 0.98 | 0.16 | 0.10 | 0.77 | 0.26 | 1.01 | 0.50 | 0.57 | 0.32 | 2.35 | 1.08 | | | 66,000 | 0.004 | 0.002 | |
| Cr | 0.11 | 0.05 | 0.01 | 0.00 | 0.03 | 0.01 | 0.06 | 0.02 | 0.02 | 0.01 | 0.11 | 0.05 | 280 | 0.10 | 1960 | 0.006 | 0.002 | |
| Mn | 1.64 | 0.83 | 0.30 | 0.14 | 0.55 | 0.19 | 0.81 | 0.41 | 0.59 | 0.37 | 1.95 | 0.97 | 4750 | 2.30 | 25,184 | 0.008 | 0.004 | |
| Fe | 75.79 | 32.16 | 5.16 | 3.09 | 28.78 | 8.94 | 32.79 | 16.05 | 19.45 | 10.36 | 80.95 | 35.30 | | 106.78 | 871,500 | 0.009 | 0.004 | |
| Ni | 0.07 | 0.03 | 0.01 | 0.00 | 0.02 | 0.01 | 0.03 | 0.01 | 0.02 | 0.01 | 0.07 | 0.03 | 190 | | 1118 | 0.007 | 0.003 | |
| Cu | 0.09 | 0.05 | 0.05 | 0.03 | 0.05 | 0.02 | 0.02 | 0.02 | 0.07 | 0.04 | 0.14 | 0.08 | 200 | 0.12 | 1140 | 0.012 | 0.007 | |
| As | 0.05 | 0.02 | 0.00 | 0.00 | 0.03 | 0.01 | 0.02 | 0.01 | 0.01 | 0.01 | 0.06 | 0.02 | | | 544 | 0.010 | 0.004 | |
| Cd | 0.0006 | 0.0003 | 0.0000 | 0.0000 | 0.0002 | 0.0001 | 0.0003 | 0.0002 | 0.0002 | 0.0001 | 0.0007 | 0.0003 | | | 23 | 0.003 | 0.001 | |
| Ba | 13.26 | 7.29 | 2.95 | 1.78 | 4.40 | 1.93 | 5.39 | 2.86 | 6.44 | 4.31 | 16.20 | 9.09 | | | 7835 | 0.207 | 0.116 | |
| Pb | 0.07 | 0.03 | 0.00 | 0.00 | 0.02 | 0.01 | 0.03 | 0.02 | 0.02 | 0.01 | 0.07 | 0.03 | | | 916 | 0.008 | 0.004 | |

from the Day River are lower than the Hong River despite concentrations of several elements suggesting D5, D6, and D7 are pollution 'hotspots'. The higher fluxes from the Hong River are likely due to higher discharge (H4 3866 $m^3/s$ in 2018 and 2612 $m^3/s$ in 2019 compared with 5032 $m^3/s$ and 3577 $m^3/s$ at the outflows). The lower discharge of the Day River reduces its capacity to transport SPM and consequently increases the potential to become a sink of deposited contaminants.

Where there is the mixing of marine and freshwaters, dissolved metal species (Fe, Mn, Al, P, Zn, Cu, Ni, Co, Pb and Mo) from river water can be transferred into suspended state (Eckert and Sholkovitz, 1976; Boyle et al., 1977; Sholkovitz, 1978; Sholkovitz et al., 1978). Higher fluxes of all particle-bound elements (except Ca) at D10 and H10 (Fig. 6) are associated with marine-influenced waters (Fig. 3), suggesting tidal influence and the increase in flux due to mixing and increased recorded discharge. During our sampling period, the marine influence only extended to H10, but other studies have monitored tidal influence up to 100 km inland (Minh et al., 2014) and with future projections of more extreme saline intrusion (Duc and Umeyama, 2011), the effects of salinity could increase the pollution of suspended sediments with toxic metals in more areas of the delta.

## 5. Conclusions

The results suggest that the contribution of heavy metals to the global oceans from the RRD are relatively small (<0.2% of global riverine elemental fluxes). However, areas of extreme pollution within the catchment are highlighted via our spatial data. Previous work in the RRD has suggested an extension in heavily polluted areas immediately surrounding Hanoi to pollution of the previously high-quality upstream section of the Day River since 2013. Results presented here suggest that the areas receiving pollution from Hanoi (D6 and D7) are extremely polluted (with EF values >40). In addition, due to rapid urbanisation and industrialisation in the catchment, upstream sections of the Hong River (e.g. H5) are also experiencing extreme pollution. Whilst reducing the amount of untreated wastewater, and therefore organic matter, entering the riverine system would limit the mobility of suspended metals, the chemical composition of inputs to the RRD would need to be monitored to assess heavy metal increase in the sediments of the delta. Furthermore, future increased monsoon intensity and saline intrusion could lead to the increased in-washing of material and the solubility of SPM-bound metals in a larger percentage of the delta, potentially leading to toxic levels of metals. Currently, on average ~50% of toxic metal flux is deposited within the delta or integrated into the riverine food web. However, increased in-washing of pollutants and future projected increases in monsoon intensity, saline intrusion, and increased human activity could shift the delta to be a source of toxic metals.

Supplementary Information

Table S1. Filtration amounts for TSS analysis

Text S1. Methods to assess the variability in flux calculation

Text S2. Methods for the categorization of enrichment factors (EFs) and EF and flux comparison with other tropical rivers.

Fig. S1. PCA biplots of elemental concentration data. Enriched elements based on SPM/UCC ratios are plotted in (A). (B) includes all measured elements and (C) includes the enriched elements alongside Ca to determine a carbonate trend and Li to determine a weathering trend. D sites are represented by the purple circles and H sites by the blue circles.

Table S2. The ratio of the elemental concentration in SPM to the upper continental crust (UCC) concentration

Table S3. Regression relationships between discharge and elemental flux on our sampling days. Relationships were used for the calculation of elemental fluxes at each sampling site for days we did not sample.

Text S3. Seasonal discharge from hydro-meteorological stations

Fig. S2. Discharge for the hydro-meteorology stations across the RRD. The corresponding sampling locations are in brackets. Discharge recorded at Nhu Tan is not located close to a sampling location and is

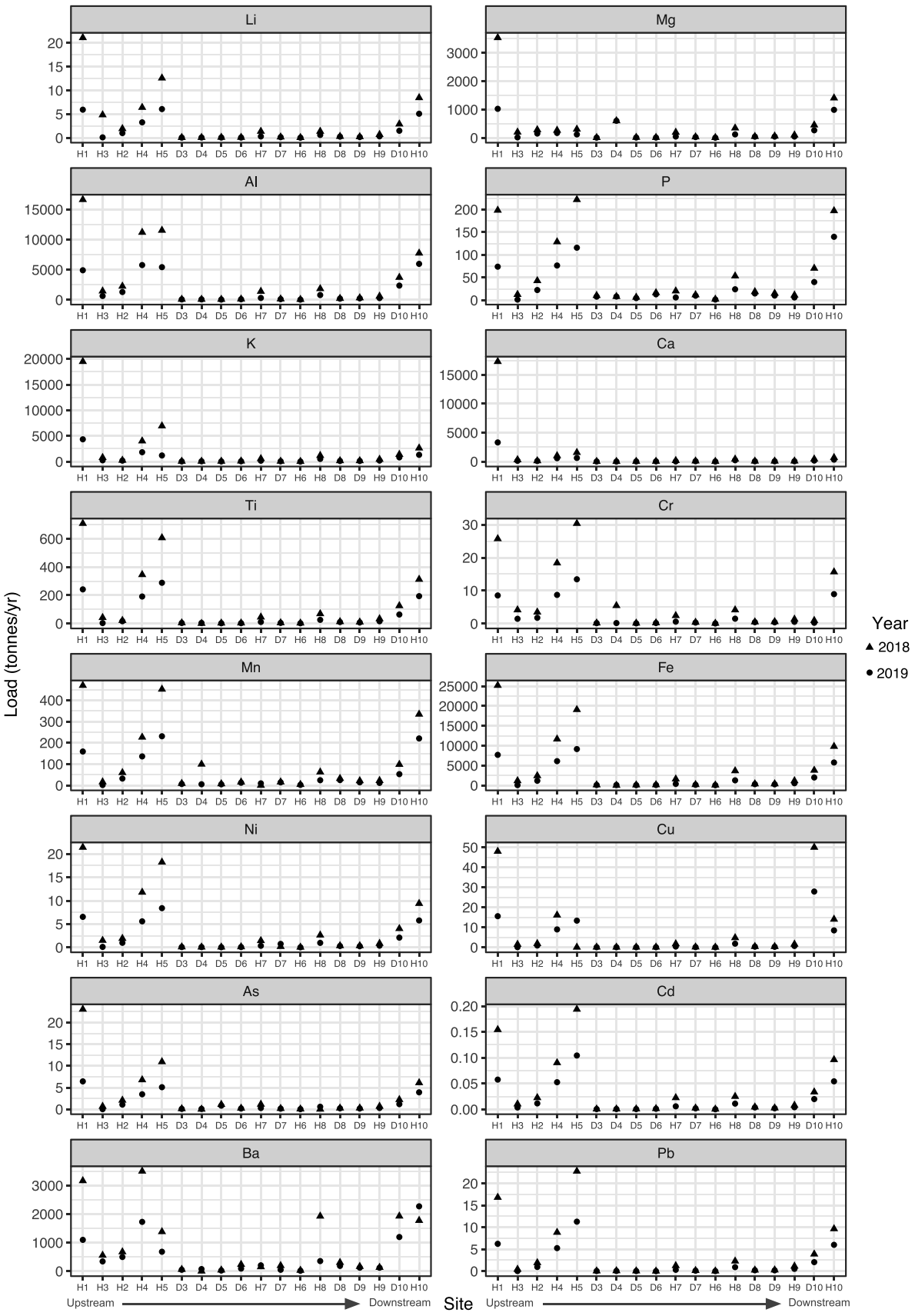


**Fig. 6.** Annual fluxes of elements in 2018 (triangles) and 2019 (circles) from upstream to downstream in the Red River Delta. Note the different y-axis scales.

**Table 5**
Annual fluxes of each element at the inflow (D6, H6, H4) and outflow (D10, H9, H10, H7, and Thuong Cat) of the Red River Delta and the percentage difference.

| Elemental Flux (Tonnes $10^3$ $yr^{-1}$) | | | | | | |
|---|---|---|---|---|---|---|
| | 2018 | | | 2019 | | |
| | Inflow | Outflow | % difference | Inflow | Outflow | % difference |
| Li | 6.53 | 15.53 | 57.95 | 3.35 | 8.27 | 59.47 |
| Mg | 285.37 | 2241.85 | 87.27 | 188.80 | 1406.46 | 86.58 |
| Al | 11,371.62 | 17,200.17 | 33.89 | 5907.67 | 10,874.70 | 45.68 |
| P | 147.11 | 341.80 | 56.96 | 90.99 | 217.36 | 58.14 |
| K | 4153.33 | 6392.37 | 35.03 | 1929.46 | 3159.42 | 38.93 |
| Ca | 1035.58 | 1670.69 | 38.01 | 602.51 | 755.57 | 20.26 |
| Ti | 351.04 | 630.68 | 44.34 | 194.79 | 346.96 | 43.86 |
| Cr | 18.72 | 26.55 | 29.48 | 8.98 | 13.34 | 32.66 |
| Mn | 246.07 | 530.61 | 53.63 | 151.41 | 340.09 | 55.48 |
| Fe | 11,879.14 | 20,269.21 | 41.39 | 6258.17 | 10,712.55 | 41.58 |
| Ni | 11.98 | 19.67 | 39.12 | 5.72 | 10.49 | 45.50 |
| Cu | 16.29 | 72.77 | 77.62 | 9.11 | 40.55 | 77.54 |
| As | 7.04 | 12.38 | 43.12 | 3.65 | 6.80 | 46.30 |
| Cd | 0.09 | 0.19 | 51.60 | 0.05 | 0.10 | 46.88 |
| Ba | 3762.75 | 5150.51 | 26.94 | 1832.09 | 4364.60 | 58.02 |
| Pb | 8.89 | 18.87 | 52.92 | 5.28 | 10.67 | 50.46 |

therefore not used in flux calculations, but is used to calculate average RRD-wide discharges. The solid line (in blue for wet season and red for dry season) represents the mean discharge and the grey shaded area shows the maximum and minimum recorded discharge. Note the different y-axis scales.

Table S4. Total suspended solid concentrations for each sampling site in the months where data for both 2018 and 2019 are available.

Text S4. Total suspended solid concentrations from hydro-meteorological stations and comparison with the monthly field collections presented in Table 2.

Table S5. Annual and seasonal total suspended solid concentrations for each hydro-meteorology station. Average concentration is calculated using the daily TSS data ($n = 365$ for annual, $n = 184$ for the wet season and $n = 181$ for the dry season). The% of months that our data falls within one standard deviation of hydro-meteorology station average monthly data is also provided.

Table S6. The difference between our field collected TSS and daily TSS recorded at hydro-meteorology stations, and the standard deviation of the hydro-meteorology data.

Text S5. Monthly concentrations of elements

Fig. S3. Plots of monthly concentrations of elements. The red line denotes dry season months, and the blue line denotes wet season months. Note the different y-axis scales. Black dashed lines represent the Vietnamese National Technical Regulation (VNTR) on Sediment Quality values for Cr, Cu, As, Cd, and Pb in freshwater and brackish water sediments (Table S3).

Table S7. Vietnamese National Technical Regulation (VNTR) on Sediment Quality values for Cr, Cu, As, Cd, and Pb in freshwater and brackish water sediments.

Fig. S4 Variability in monthly elemental flux using hydro-meteorology station daily TSS and monthly field collected TSS. This was calculated for March 2018 to July 2019 to cover the period of our field campaign. The calculation was not applied to elements or sites where elemental data were below detection limit. The comparisons are only possible for H1, H2, H3, H5 and H10 due to the availability of hydro-meteorology station TSS data. The grey circles represent the daily flux calculated using the daily MONRE TSS data and the black circles represent the monthly mean of this data. The orange circles represent the monthly mean if daily flux is calculated using the monthly field collected TSS. The black and orange error bars represent one standard deviation of the mean.

## Declaration of Competing Interest

The authors declare that they have no known competing financial interests or personal relationships that could have appeared to influence the work reported in this paper.

## Data Availability

Data will be made available on request.

## Acknowledgments

This work was funded by NERC-NAFOSTED Research Partnerships grant NE/P014577/1 and supported by funding from the UKRI-GCRF Living Deltas Hub (NE/S008926/1). The authors thank two anonymous reviewers for their thoughtful comments, which helped to improve the manuscript.

## Supplementary materials

Supplementary material associated with this article can be found, in the online version, at doi:10.1016/j.watres.2022.119053.

## References

Agusa, T., Inoue, S., Kunito, T., Kubota, R., Minh, T.B., Trang, P.T.K., Subramanian, A., Iwata, H., Viet, P.H., Tanabe, S., 2005. Widely-distributed arsenic pollution in groundwater in the Red River Delta. Vietnam Biomed. Res. Trace Ele. 16, 296–298.
American Public Health Association, 2017. Standard Methods for the Examination of Water and Wastewater. American Public Health Association, Washington D.C.
Boyle, E., Edmond, J., Sholkovitz, E., 1977. The mechanism of iron removal in estuaries. Geochim. Cosmochim. Acta 41, 1313–1324.
Carvalho, C.E.V., Salomão, M.S.M.B., Molisani, M.M., Rezende, C.E., Lacerda, L.D., 2002. Contribution of a medium-sized tropical river to the particulate heavy-metal load for the South Atlantic Ocean. Sci. Total Environ. 284, 85–93.
Clesceri, L.S., Greenberg, A.E., Eaton, A.D., 1999. Standard Methods for the Examination of Water and Wastewater, 20th. APHA, Washington D.C.
Dai, A., Trenberth, K.E., 2002. Estimates of freshwater discharge from continents: latitudinal and seasonal variations. J. Hydrometeorol.y 3, 660–687.
Davies, R. 2018. Vietnam – storm 'Son Tinh' causes deadly floods and landslides. *Floodlist.* Available at: https://floodlist.com/asia/vietnam-storm-son-tinh-july-2018; accessed 18/02/22.
Do, T.N., Nishida, K., 2014. A nitrogen cycle model in paddy fields to improve material flow analysis: the Day-Nhue River Basin case study. Nutr. Cycl. Agroecosyst. 100, 215–226.
Do, T.N., Tran, V.B., Trinh, A.D., Nishida, K., 2019. Quantification of nitrogen load in a regulated river system in Vietnam by material flow analysis. J. Mater. Cycles Waste Manage. 21, 974–983.
Duc, N.H., Umeyama, M., 2011. Saline intrusion due to the accelerative sea level in the Red River system in Vietnam. In: Beighley, E., Killgore, M.W. (Eds.), World Environmental and Water Resources Congress 2011: Bearing Knowledge for Sustainability, eds., pp. 4413–4422.
Dupré, B., Gaillardet, J., Rousseau, D., Allègre, C.J., 1996. Major and trace elements of river-borne material: the Congo Basin. Geochim. Cosmochim. Acta 60, 1301–1321.
Eckert, J., Sholkovitz, E., 1976. The flocculation of iron, aluminium and humates from river water by electrolytes. Geochim. Cosmochim. Acta 40, 847–848.

Environmental Police Agency, 2009. Scientific Report on Preventing and Fighting Against the Violation of The Environmental Protection Law in Craft Villages. EPA (Vietnam Environmental Police Agency), Hanoi.
Ericson, J.P., Vörösmarty, C.J., Dingman, S.L., Ward, L.G., Meybeck, M., 2006. Effective sea-level rise and deltas: causes of change and human dimension implications. Glob. Planet. Change 50, 63–82.
General Statistic Office, 2017. Statistical Handbook of Vietnam. Statistical Publisher, Hanoi.
General Statistic Office, 2018. Statistical Handbook of Vietnam. Statistical Publisher, Hanoi.
General Statistic Office, 2020. Statistical Handbook of Vietnam. Statistical Publisher, Hanoi.
Ha, D.T., Coynel, A., 2016. River hydrology and recent suspended sediment flux in the Red River: implication for assessing soil erosion and sediment transport/deposition processes. Vietnam J. Sci. Technol. 54, 614.
Ha, V., Vu, T., 2012. Analysis of the effects of the reservoirs in the upstream Chinese section to the lower section flow of the Da and Thao Rivers. J. *Water Res. Environ. Eng* 38, 3–8.
Hori, K., 2021. Deltas. *Reference Module in Earth Systems and Environmental Sciences*. Elsevier, Amsterdam.
Hu, Z., Gao, S., 2008. Upper crustal abundances of trace elements: a revision and update. Chem. Geol. 253, 205–221.
Jenne, E.A. 1968. Controls on Mn, Fe, Co, Ni, Cu, and Zn concentrations in soils and water: the significant role of hydrous Mn and Fe Oxides. *In*: Baker R.A. (Ed.) Trace Inorganics in Water.Miami, FL: American Chemical Society. 21, 337–387.
Le, N.D., Le, T.P.Q., Phung, T.X.B., Duong, T.T., Didier, O., 2020. Impact of hydropower dam on total suspended sediment and total organic nitrogen fluxes of the Red River (Vietnam). Proc. IAHS 383, 367–374.
Le, T.P.Q., Marchand, C., Ho, C.T., Le, N.D., Duong, T.T., Lu, X., Doan, P.K., Nguyen, T. K., Nguyen, T.M.H., Vu, D.A., 2018. CO2 partial pressure and CO2 emission along the lower Red River (Vietnam). Biogeosciences 15, 4799–4814.
Luu, T.N.M., Do, T.N., Matiatos, I., Panizzo, V.N., Trinh, A.D., 2020. Stable isotopes as an effective tool for N nutrient source identification in a heavily urbanized and agriculturally intensive tropical lowland basin. Biogeochemistry 149, 17–35.
Luu, T.N.M., Garnier, J., Billen, G., Le, T.P.Q., Nemery, J., Orange, D., Le, L.A., 2012. N, P, Si budgets for the Red River Delta (northern Vietnam): how the delta affects river nutrient delivery to the sea. Biogeochemistry 107, 241–259.
Luu, T.N.M., Garnier, J., Billen, G., Orange, D., Némery, J., Le, T.P.Q., Tran, H.T., Le, L. A., 2010. Hydrological regime and water budget of the Red River Delta (Northern Vietnam). J. Asian Earth Sci. 37, 219–228.
Maavara, T., Chen, Q., Van Meter, K., Brown, L.E., Zhang, J., Ni, J., Zarfl, C., 2020. River dam impacts on biogeochemical cycling. Nature Rev. Earth Environ. 1, 103–116.
Mahanty, S., Dang, T.D. & Gianghai, P. 2012. Crafting sustainability: managing water pollution in Viet Nam's craft villages *Development Policy Centre Discussion Paper No. 20*, Available at SSRN: https://ssrn.com/abstract=2094814.
Martin, J.-.M., Whitfield, M., 1983. The Significance of the river input of chemical elements to the ocean. In: Wong, C.S., Boyle, E., Bruland, K.W., Burton, J.D., Goldberg, E.D. (Eds.), Trace Metals in Sea Water, eds. Springer US, Boston, MA.
Mclennan, S.M., 2001. Relationships Between the Trace Element Composition of Sedimentary Rocks and Upper Continental Crust. Geochemistry, Geophysics, Geosystems, p. 2.
Minh, L.T.N., Orange, D., Thai, T.H., Garnier, J., Trinh, A.D., et al., 2014. Hydrological regime of a tidal system in the Red River Delta, northern Vietnam. In: Daniell, T.M., Van Lanen, H.A.J., Demuth, S., Laaha, G., Servat, E., Mahé, G., et al. (Eds.), Hydrology in a Changing world: Environmental and Human Dimensions, eds. AISH, Wallingford, pp. 451–456.
Mitra, A., Ghosh, R., 2014. Bioaccumulation pattern of heavy metals in commercially important fishes in and around Indian Sundarbans. Glob. J. Anim. Sci. Res. 2, 33–44.
MONRE, 2008. Environment report of Vietnam. 2008. Craft Village Environment'/'Bao Cao Moi Truong Quoc Gia 2008: Moi Truong Lang Nghe VietNam. MONRE (Ministry of National Resources and Environment), Hanoi.
Murillo, V.C., Silva, C.G., Fernandez, G.B., 2009. Nearshore sediments and coastal evolution of Paraíba do Sul River delta. Rio de Janeiro, Brazil J. Coastal Res. 650–654.
Ngo, H.T.T., Tran, L.A.T., Nguyen, D.Q., Nguyen, T.T.H., Le, T.T., Gao, Y., 2021. Metal Pollution and Bioaccumulation in the Nhue-Day River Basin, Vietnam: potential Ecological and Human Health Risks. Int. J. Environ. Res. Public Health 18, 13425.
Nguyen, N.L., Do, T.N., Trinh, A.D., 2021. Application of water stable isotopes for hydrological characterization of the red river (Asia). Water (Basel) 13, 2051.
Ovalle, A., Silva, C., Rezende, C.D., Gatts, C., Suzuki, M., Figueiredo, R., 2013. Long-term trends in hydrochemistry in the Paraíba do Sul River, southeastern Brazil. J. Hydrol. (Amst.) 481, 191–203.
Quynh, L.T.P., Billen, G., Garnier, J., Théry, S., Fézard, C., Minh, C.V., 2005. Nutrient (N, P) budgets for the Red River basin (Vietnam and China). Glob. Biogeochem. Cycles 19.
Redman, A.D., Macalady, D.L., Ahmann, D., 2002. Natural organic matter affects arsenic speciation and sorption onto hematite. Environ. Sci. Technol. 36, 2889–2896.
Roy, D., Pramanik, A., Banerjee, S., Ghosh, A., Chattopadhyay, D., Bhattacharyya, M., 2018. Spatio-temporal variability and source identification for metal contamination in the river sediment of Indian Sundarbans, a world heritage site. Environ. Sci. Pollut. Res. 25, 31326–31345.
Rudnick, R.L. and Gao, S. (2003) The composition of the continental crust. In: Holland, H.D. and Turekian, K.K., Eds., Treatise On Geochemistry, Vol. 3, The Crust, Elsevier-Pergamon, Oxford, 1–64.
Samanta, S., Dalai, T.K., 2018. Massive production of heavy metals in the Ganga (Hooghly) River estuary, India: global importance of solute-particle interaction and enhanced metal fluxes to the oceans. Geochim. Cosmochim. Acta 228, 243–258.
Shafer, M.M., Overdier, J.T., Hurley, J.P., Armstrong, D., Webb, D., 1997. The influence of dissolved organic carbon, suspended particulates, and hydrology on the concentration, partitioning and variability of trace metals in two contrasting Wisconsin watersheds (USA). Chem. Geol. 136, 71–97.
Sholkovitz, E.R., 1978. The flocculation of dissolved Fe, Mn, Al, Cu, NI, Co and Cd during estuarine mixing. Earth Planet. Sci. Lett. 41, 77–86.
Sholkovitz, E., Boyle, E., Price, N., 1978. The removal of dissolved humic acids and iron during estuarine mixing. Earth Planet. Sci. Lett. 40, 130–136.
Subramanian, V., Van Grieken, R., Van't Dack, L., 1987. Heavy metals distribution in the sediments of Ganges and Brahmaputra rivers. Environ. Geol. Water Sci. 9, 93.
Sutherland, R., 2000. Bed sediment-associated trace metals in an urban stream. Oahu, Hawaii Environ. Geol. 39, 611–627.
Taylor, S.R. & Mclennan, S.M. 1985. The continental crust: its composition and evolution.
Tran, T.X., 2007. Hydrological Characteristic and Water Resources in Vietnam, Agricultural Ed. Hanoi, p. 427.
Trinh, A.D., Giang, N.H., Vachaud, G., Choi, S.U., 2009. Application of excess carbon dioxide partial pressure (EpCO2) to the assessment of trophic state of surface water in the Red River Delta of Vietnam. Int. J. Environ. Stud. 66, 27–47.
Trinh, A.D., Loi, V.D., Thao, T.T., 2013. Partition of heavy metals in a tropical river system impacted by municipal waste. Environ. Monit. Assess. 185, 1907–1925.
Turner, A., 1996. Trace-metal partitioning in estuaries: importance of salinity and particle concentration. Mar. Chem. 54, 27–39.
Viers, J., Dupré, B., Gaillardet, J., 2009. Chemical composition of suspended sediments in World Rivers: new insights from a new database. Sci. Total Environ. 407, 853–868.
Warren, L.A., Zimmerman, A.P., 1994. The importance of surface area in metal sorption by oxides and organic matter in a heterogeneous natural sediment. Appl. Geochem. 9, 245–254.
Woodroffe, C.D., Nicholls, R.J., Saito, Y., Chen, Z., Goodbred, S.L., 2006. Landscape Variability and the Response of Asian Megadeltas to Environmental change. *Global change and Integrated Coastal Management*. Springer, Berlin.
Bank, World, 2008. Review and Analysis of the Pollution Impacts from Vietnamese Manufacturing Sectors. The World Bank: East Asia & Pacific Region/Sustainable Development Department.
Wright, P., 2018. Flooding, Mudslides Triggered by Tropical Storm Son Tinh Kill at Least 10 in Vietnam. The Weather Channel. Available at. https://weather.com/news/news/2018-07-21-vietnam-storm-typhoon-son-tinh. accessed 18/02/22.
Zhang, J., Zhou, F., Chen, C., Sun, X., Shi, Y., Zhao, H., Chen, F., 2018. Spatial distribution and correlation characteristics of heavy metals in the seawater, suspended particulate matter and sediments in Zhanjiang Bay. China PLoS ONE 13, e0201414.